

# Bound States and Universality in Layers of Cold Polar Molecules

J. R. ARMSTRONG<sup>1</sup>, N. T. ZINNER<sup>1,2</sup>, D. V. FEDOROV<sup>1</sup> and A. S. JENSEN<sup>1</sup>

<sup>1</sup> *Department of Physics and Astronomy - Aarhus University, Ny Munkegade, byg. 1520, DK8000 Århus C, Denmark*

<sup>2</sup> *The Niels Bohr Institute, Blegdamsvej 17, DK-2100 Copenhagen Ø, Denmark*

PACS 67.85.-d – Ultracold gases, trapped gases

PACS 36.20.-r – Macromolecules and polymer molecules

PACS 05.30.-d – Quantum statistical mechanics

**Abstract.** – The recent experimental realization of cold polar molecules in the rotational and vibrational ground state opens the door to the study of a wealth of phenomena involving long-range interactions. By applying an optical lattice to a gas of cold polar molecules one can create a layered system of planar traps. Due to the long-range dipole-dipole interaction one expects a rich structure of bound complexes in this geometry. We study the bilayer case and determine the two-body bound state properties as a function of the interaction strength. The results clearly show that a least one bound state will always be present in the system. In addition, bound states at zero energy show universal behavior and extend to very large radii. These results suggest that non-trivial bound complexes of more than two particles are likely in the bilayer and in more complicated chain structures in multi-layer systems.

**Introduction.** – Quantum gases of polar atoms and molecules in their rovibrational ground-state represent a unique opportunity to study the interplay of long- and short-range interactions in the highly controllable trapped gas environment. Early experiments used magnetic dipolar atoms [1–4] which have observable effects in spite of intrinsically weak dipole moments. Recently, heteronuclear molecules with very large electric dipole moments have been realized by a number of groups [5–9]. The goal of a quantum degenerate system of polar molecules with strong  $1/r^3$  long-range dipole-dipole forces therefore seems close at hand.

The attractive force of polar molecules in the head-to-tail configuration can lead to collapse of the system [10]. However, as suggested by Wang et al. [11], a one-dimensional optical lattice that creates a multilayered stack of pancake systems can stabilize the situation. If we apply a field to polarize the dipole perpendicular to the layers then the intralayer interaction will be purely repulsive, whereas the interlayer part will be attractive but with the optical lattices separating the dipoles in different layers. This setup is presently being implemented experimentally. As discussed in [11], the dipole-dipole force forms bound chains and the system effectively behaves as a liquid of chains with resemblance to rheological fluids. In the case of bosons we expect the chains to Bose condense at low temperatures. However, if we have fermionic polar

molecules the situation is less clear since one would expect a Bose-Fermi mixtures with various bound complexes [12].

If we simplify the problem to consider just two adjacent layers we have a system with  $1/r^3$  interactions that mimics the long-range  $1/r$  interactions in graphene [13] and semiconductor bilayers [14]. In the semiconductor case bound states of exciton pairs with non-zero dipole moments have been considered in connection with organic interfaces and quantum wells [15]. For small coupling strength it was concluded that no bound state exists [15]. This was also stated in several recent works concerning cold polar molecules [11, 12, 16] where the conclusion was based on a Gaussian ansatz. However, at small coupling the particles are strongly delocalized and a localized Gaussian is therefore not a good approximation [17]. To make matters worse, the potential integrates to zero over the plane and thus at small coupling the Landau criterion [18] for a bound state in two-dimensional systems is not applicable. Using scattering theory it was recently shown that a bound state presumably exists for arbitrarily small moments [19, 20]. However, the scattering theory is intricate and does not yield straightforward information about the behavior of the two-body bound state wave function.

The purpose of the present work is to compute and explain the basic properties of two-body systems used as the fundamental building blocks for layered dipolar structures. We shall employ simple model potentials to extract

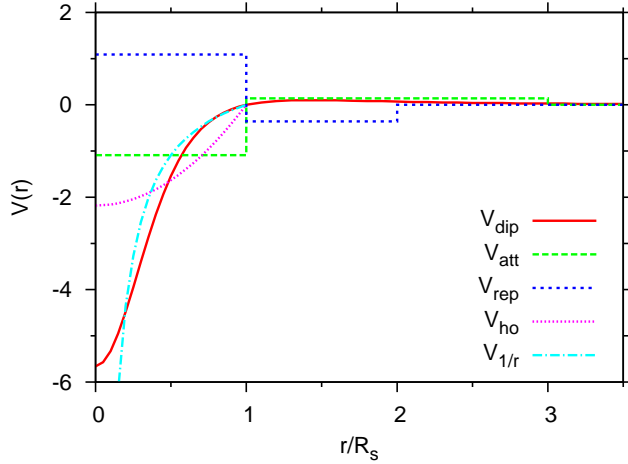


Fig. 1: Dipole-dipole potential,  $V_{dip}$ , along with two model square well potentials and two other alternatives for an initial attractive well, a harmonic oscillator potential,  $V_{ho}$  and  $1/r$  potential,  $V_{1/r}$ . Both square well potentials have the same attractive and repulsive volumes as the dipole-dipole potential.  $V_{att}$  is the initial attractive well configuration,  $V_{rep}$  has the sign flipped by having the barrier first, and a different  $R_l$ . All potentials have the same volume.

universal properties, point out where details of the potentials are needed, and illustrate relations between wave functions, energies, and radii. We shall use square well, harmonic oscillator and  $1/r$ -potentials in two dimensions, and compare to solutions of the true dipole-dipole potential. We briefly sketch the model solutions, discuss the energies, the threshold properties, and various immediate implications.

**Model solutions.** – We solve the 2 dimensional (2D) Schrödinger equation, which is possible to do analytically with several model potentials. We use cylindrical coordinates  $(r, \theta)$  and separate the total wave function  $\Psi = R(r)\Phi(\theta)$  into radial  $R(r)$  and angular  $\Phi(\theta)$  parts. With  $\Phi(\theta) = \exp(im\theta)/\sqrt{2\pi}$ , where  $m$  is an integer, the stationary radial Schrödinger equation becomes:

$$\left[ -\frac{\hbar^2}{2m} \left( \frac{d^2}{dr^2} + \frac{1-m^2}{4r^2} \right) + V(r) \right] u(r) = Eu(r), \quad (1)$$

where  $u = \sqrt{r}R(r)$  is the reduced radial wave function,  $E$  is the energy, and  $V(r)$  is the potential, assumed to be spherically symmetric. We consider potentials with net volume equal to zero,  $\int V(r)d^2r = 0$ , as for the dipole-dipole potential, i.e.

$$V(r) = D^2 \frac{r^2 - 2d^2}{(r^2 + d^2)^{5/2}}, \quad (2)$$

where  $D$  is the electric dipole moment and  $d$  is the distance between the two different layers containing the particles. To visualize we show this potential in Fig. 1 in comparison with square well, harmonic oscillator, and  $1/r$  potentials

at distances less than  $R_s \equiv d\sqrt{2}$ . For larger distances the volume conserving condition dictates the strength for a given form. For the square well shape where the small,  $V_s$ , and large,  $V_l$ , distance strengths both chosen positive are related by

$$\frac{V_s}{V_l} = \left( \frac{R_l}{R_s} \right)^2 - 1, \quad (3)$$

where  $R_l$  is the radius where the outer square well ends. The inner part is the most interesting and we shall only match the different potentials with the square barrier shape for  $r > R_s$ .  $D^2$  is related to  $V_s$  by  $D^2 = V_s R_s^3 (3/2)^{3/2} / 2$ .

One of our main concerns is the appearance of a bound state at small couplings. We therefore consider the  $m = 0$  case here. The general  $m$  case can be analyzed in a similar fashion. Then Eq. (1) simplifies in general to

$$\frac{d^2 u}{dr^2} + \left( \frac{1}{4r^2} - k^2 \right) u = 0, \quad (4)$$

where  $k^2 = 2m(E - V(r))/\hbar^2$  depends on  $r$ .

Let us now first solve completely the piecewise constant potential in Fig. 1 for use as a reference standard. Then the wave functions in the three different regions of space are the Riccati Bessel functions of order  $-1/2$ , which means that the solutions for  $R(r)$  are various Bessel functions of order 0 depending on region of space:

$$R = \begin{cases} AJ_0(k_1 r) & r \leq R_s \\ BI_0(k_2 r) + CK_0(k_2 r) & R_s < r \leq R_l \\ DK_0(k_3 r) & r > R_l, \end{cases} \quad (5)$$

where  $J_0(kr)$  is the Bessel function,  $I_0(kr)$  and  $K_0(kr)$  are the modified Bessel functions of the first and second kind, respectively, and the coefficients  $A, B, C$ , and  $D$  are to be determined by matching at the region boundaries and normalization. The wavenumbers,  $k_i$ , are the absolute values of  $\mathbf{k}$  in the regions. Matching logarithmic derivatives leads to the transcendental equation for the energies:

$$\frac{k_2 R_l K_0(k_3 R_l) K_1(k_2 R_l) - k_3 R_l K_0(k_2 R_l) K_1(k_3 R_l)}{k_3 R_l I_0(k_2 R_l) K_1(k_3 R_l) + k_2 R_l K_0(k_3 R_l) I_1(k_2 R_l)} = \frac{k_2 R_s J_0(k_1 R_s) K_1(k_2 R_s) - k_1 R_s K_0(k_2 R_s) J_1(k_1 R_s)}{k_2 R_s J_0(k_1 R_s) I_1(k_2 R_s) + k_1 R_s I_0(k_2 R_s) J_1(k_1 R_s)}. \quad (6)$$

This formula and the wave function, Eq.(5), are valid when for the potential  $V_{att}$  in Fig. 1. For  $V_{rep}$  from Fig. 1, one merely takes the analytic continuation of the relevant Bessel function, which can be found in, for example [22].

Analytic solutions can also be found when the short-distance part of the potential is substituted by a harmonic oscillator potential,  $V_{ho}(r) = 2V_s[(r/R_s)^2 - 1]$  and a  $1/r$  potential,  $V_{1/r}(r) = V_s(1 - R_s/r)$ . In both cases the potentials are zero for  $r = R_s$  and  $V_s$  is the strength of the box potential with the same volume. Note that the harmonic oscillator is shifted down and the  $1/r$  potential is shifted up.

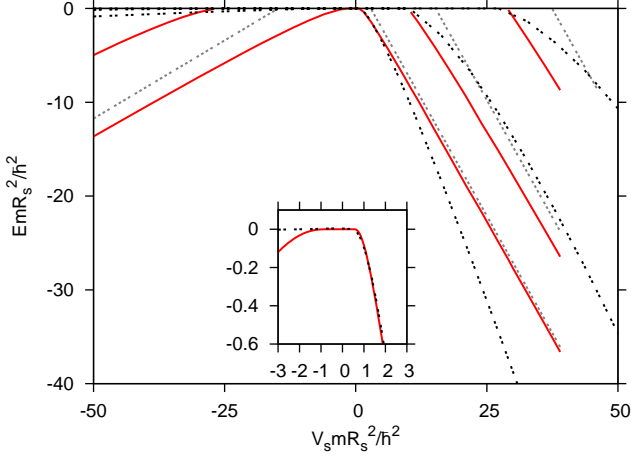


Fig. 2: Energies of states as a function of  $V_s$  in units of  $\hbar^2/(mR_s^2)$ . Right and left correspond to  $V_{att}$  and  $V_{rep}$ , respective, of Fig. 1, and  $R_l = 2R_s$ . The dotted red lines are the calculated asymptotic values for the ground, first, and second excited states, the solid red dotted lines the square well energies, and the black double-dotted line the dipole-dipole potential results. Insert is a zoom of small energy.

The radial wave functions for  $r < R_s$  are given by  $R(r) = N \exp(-z/2)M$ , where  $M$  is the confluent hypergeometric function, or Kummer function  $M(a, b, z)$  with three arguments. We have  $b = 1$  and  $a$  and  $z$  are:

$$a = \frac{1}{2} - \frac{E + 2V_s}{4\hbar} \sqrt{\frac{mR_s^2}{V_s}}, \quad z = \frac{2r^2 \sqrt{mV_s}}{\hbar R_s} \quad (7)$$

$$a = \frac{1}{2} - \frac{R_s V_s}{\hbar} \sqrt{\frac{m}{2(V_s - E)}}, \quad z = \frac{r \sqrt{8m(V_s - E)}}{\sqrt{\hbar^2}} \quad (8)$$

for oscillator and  $1/r$  potentials, respectively. This is the solution vanishing at  $r = 0$ . Matching at  $r = R_s$  with the solutions for  $r < R_s$  leads to transcendental equations for the energies.

**Energies.** — The energies obtained from Eq. (6) are shown in Fig. 2 as function of  $V_s$ , or equivalently of volume of either attraction or repulsion. We choose  $R_l = 2R_s$  and use  $V_l$  from Eq.(3). We see that at least one bound state is always present for *any* non-zero attractive potentials even when the strength is approaching zero. The numerical results for the dipole potential coincide with the square well at small energies. As the attractive part of the potential becomes deeper, and correspondingly also the repulsive part, more states appear. This is understandable as sufficiently deep potentials always bind a particle independent of confining barriers. It follows furthermore from the fact that the attractive “centrifugal” barrier in itself only needs an additional infinitesimal attraction to bind. If that attraction is an increase of the negative centrifugal strength infinitely many bound states appear.

Increasing  $V_s$  then leads to more bound states which more and more are determined from the attraction alone.

The condition,  $J_0(k_1 R_s) = 0$ , determines  $k_1$  for  $V_{att}$  in Fig. 1 and thereby the bound state energy  $E_n$  is related to the nodes of the Bessel function, i.e.

$$E_n = -V_s + \frac{\hbar^2(j_{0,n})^2}{2mR_s^2}, \quad (9)$$

where  $j_{0,n}$  is the  $n$ th zero of  $J_0(x)$ . This asymptotic limit of straight lines of slope equal to one is valid for an infinitely high barrier. The ground state is the deepest and agrees well with the asymptotic limit, but for the excited states the well must be deeper to reach the limit, around -150 for 1% agreement for the first excited state.

For  $V_{rep}$  in Fig. 1, where the repulsion is for  $r < R_s$  and the attractive well is at  $R_s < r < R_l$ , no confining barrier exists at larger distance. Here, the bound state wave function is  $R(r) = AJ_0(r) + BN_0(r)$ , where  $N_0(r)$  is the Neumann function. In the deep well limit, the wave function must vanish at both endpoints where large energy implies large arguments of both the Bessel and Neumann functions. Then  $k_2^2(R_l - R_s)^2 = n^2\pi^2$  or equivalently

$$E_n = -\frac{V_s}{(R_l/R_s)^2 - 1} + \frac{n^2\pi^2\hbar^2}{2m(R_l - R_s)^2}, \quad (10)$$

where the slopes of the lines are dependent on  $R_l$  and therefore different from the  $V_{att}$  case. These estimates are much further off than the similar estimates for  $V_{att}$ . For the difference between the energies and the estimate to be 1% for the ground state, the depth of the well needs to be around 100. For that level of agreement in the first excited state, the well depth needs to be around 250.

These computations are also carried out for harmonic oscillator and  $1/r$  potentials instead of the attractive square well at short distance. The condition for deeply bound states is that the wave function must vanish exponentially with  $r$ . This implies that the first argument  $a$  of the Kummer function must be a non-positive integer  $-n$  counting the number of bound states. Then  $M$  reduces to the Laguerre polynomials. The energies become

$$E_{ho} = 2[-V_s + \sqrt{\frac{V_s \hbar^2}{mR_s^2}}(2n + 1)], \quad (11)$$

$$E_{1/r} = V_s - \frac{2mV_s^2 R_s^2}{\hbar^2(2n + 1)^2}, \quad (12)$$

where  $n$  can take the values 0,1,2, etc. These energies are only approached asymptotically as for the square well in Fig. 1. They are as suspected highly potential dependent for well-bound states as shown in Fig. 3. This is understandable as the barrier essentially has no influence on these energies. The potential in Eq.(2) leads to energies between those of harmonic and  $1/r$  potentials. Thus limits to realistic potentials can be provided by analytic models.

However, in the limit where  $V_s \rightarrow 0$  both energies in Eqs.(11) and (12) approach zero from positive values. This is due to the approximations where the solutions

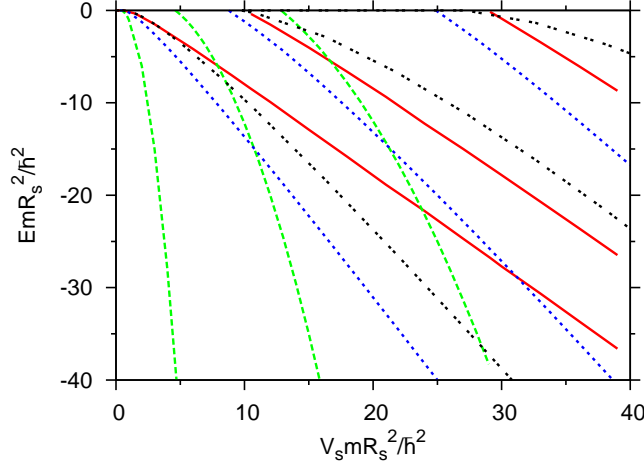


Fig. 3: Bound state energies for the ground state and first two excited states as a function of potential well depth for the three model and the dipole-dipole potentials. The solid red lines are the square well states, the dashed blue lines are from a harmonic oscillator well, the dashed green lines from a  $1/r$ -type potential, and the black double-dotted lines from the dipole-dipole potential (only the ground state and first excited state are shown for this potential). The square well barrier is the same in all cases, and  $R_l = 2R_s$ .

are obtained from the potentials maintaining their harmonic oscillator and  $1/r$  behavior for all distances including  $r > R_s$ . Thus the repulsive barrier is strongly exaggerated compared to the square well barrier corresponding to zero net volume. Using these more appropriate square well barriers we find numerically that the correct energies for both potentials always remain negative corresponding to bound states for all values of  $V_s$ . This conclusion is confirmed numerically for the dipole-dipole potential in Eq.(2). Thus potentials with zero net volume always have at least one bound state in two dimensions.

**Threshold properties.** — The weakly bound states often reveal unique physics as for example Efimov and halo states with universal properties. The number of nodes as function of volume can be found rather precisely from Eqs.(9), (11) and (12) by solving for  $n$  with  $E_n = 0$ . The explicit result for harmonic oscillator,  $2n + 1 = \sqrt{m|V_s|R_s^2/\hbar}$ , whereas for the  $1/r$  potential the right-hand side is a factor  $\sqrt{2}$  larger. Thus these potentials would have the same number of bound states if the volume of the oscillator were twice as large as that of the  $1/r$ -potential. The dipole-dipole potential seems from Fig. 1 to have intermediate properties. However, the dependencies on strength for each energy differs substantially, see Eqs.(11) and (12).

The same extrapolation to the threshold can be applied to the wave functions. We then find that the mean square radius is given as  $\langle r^2 \rangle / R_s^2 = 1/2$  for the oscillator and  $5/8$  to leading order for the  $1/r$  potential. These threshold radii, obtained from asymptotic strong binding, are

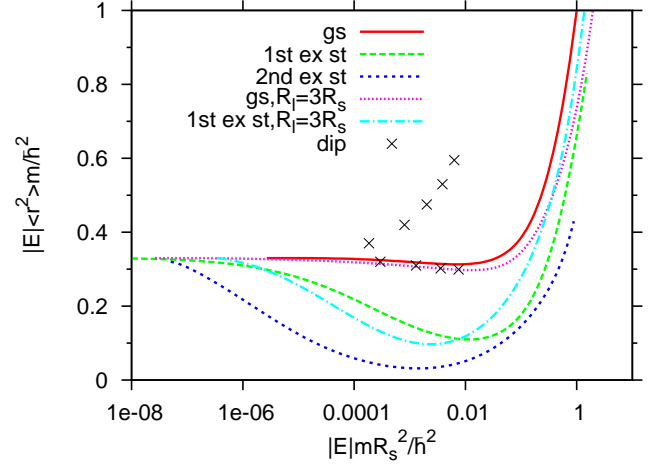


Fig. 4: Binding energy multiplied with  $\langle r^2 \rangle$  plotted against the binding energy for the ground state and first two excited states in the  $R_l = 2R_s$  system, and for the ground and first excited state for the  $R_l = 3R_s$  system. Also plotted (with points) are the results for the dipole-dipole potential. The lines approaching the asymptotic limit from the bottom are from the  $V_{att}$  potential in Fig. 1, while those approaching from above are coming from the  $V_{rep}$  potential. Note that the abscissa scale is logarithmic, with small binding energies to the left.

however qualitatively completely wrong when the energy is sufficiently close to zero. In Fig. 2 the straight lines approaching zero bend over as the system attempts to stay bound for a weaker potential. The wave function is correspondingly leaking out under the barrier as the energy approaches zero. This is the effect producing nuclear halos [17] where the mean square radius for two particles in three dimensions becomes inversely proportional to the energy. The analogue here is that most of the probability is found for  $r > R_l$  where the wave function is  $K_0$ . This means that the mean square radius then approaches [21]

$$\langle r^2 \rangle = \frac{\hbar^2}{2m|E|} \frac{\int_0^\infty x^3 |K_0(x)|^2 dx}{\int_0^\infty x |K_0(x)|^2 dx} = \frac{1}{3} \frac{\hbar^2}{m|E|}, \quad (13)$$

which is a universal result independent of both the particular ( $s$ -wave) state considered and the shape of the attractive potential.

The rate of approach to the asymptotic value in Eq.(13) is seen in Figure 4 where we show the product of the binding energy and the radius squared against the binding energy. Large binding energies correspond to wave functions located in the attractive well. As the threshold is approached the wave function begins to leak out and eventually ends up in the universal limit in Eq.(13), where details of the potential are unimportant. However, how that limit is approached depends on the presence of a barrier. Without a barrier ( $V_{rep}$  from Fig. 1), all states, both ground and excited, approach the weak binding limit in the same way. This is precisely the halo effect [17].

The similar approach to universality is found for the

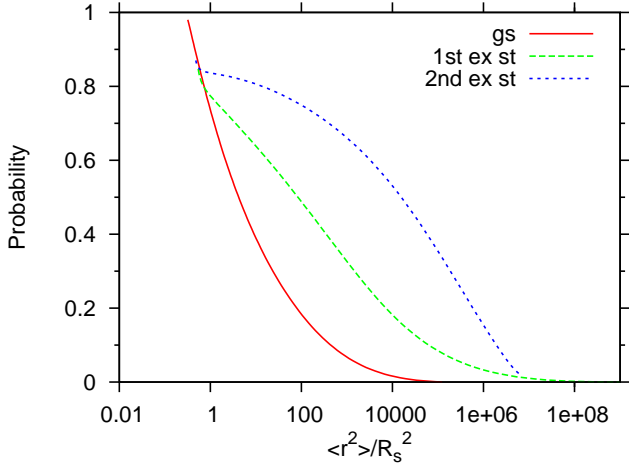


Fig. 5: The probability,  $\int_0^{R_s} |u|^2 dr$ , of finding the particle inside of the attractive part of the  $V_{att}$  potential as a function of  $\langle r^2 \rangle$ . The ground state and first two excited states of the  $R_l = 2R_s$  system are shown. For  $V_{rep}$ , all states behave as the ground states of both potentials.

ground state for  $V_{att}$  from Fig. 1 since then the barrier vanishes with the binding energy. For excited states of  $V_{att}$ , the barrier remains finite for vanishing binding energy. High excitation goes together with high barrier which causes even the weakly bound states to remain localized in the attractive region. The approach to universality is delayed by many orders of magnitude in binding energy. During the approach the radius remains small for small energies and consequently the curves dive below the universal limit before the eventual approach. These features become more pronounced with excitation energy. Numerical solutions for these small energies are very difficult to compute.

In Figure 4 we also show results for different values of  $R_l$ , still with  $V_l$  adjusted to maintain zero net volume. The curves for the ground states are roughly identical. This is also seen at higher energies for the first excited state, but eventually at small energies a wider barrier delays the escape of the wave function even though the barrier is correspondingly smaller.

The rate of approach to the universal limit at threshold is further illustrated in Figure 5. The probability distribution from the wavefunction is moving slower than the distribution in the mean square radius integral. An example is that the bulk of the probability can stay in the attractive well while the root mean square radius is much larger than the radius of the attraction. Thus the tail properties are crucial. Again these effects are enhanced for excited states because the final expulsion of the wave function to the external region comes much later for the excited states constraint by a large barrier.

The formal connection is that the wave function essentially is  $J_0$  until the energy is very small where it has to change to  $K_0$ , see Eq.(5). Computation of mean square ra-

dius then employs  $J_0$  for normalization but  $K_0$  for the  $r^2$ -distribution. Thus neither short nor large-distance properties are sufficient for a description in this transition region.

**Implications for many particles.** – Several conclusions are immediately deduced from our model systems. First of all at least one bound state must appear in 2D for any potential with zero net volume. Thus, in contrast to the statements in [11, 12, 15, 16], one bound state is always present in a bilayer with dipoles oriented perpendicular to the layers. This in turn means that arguments based on the existence of a critical strength for binding should be re-considered. Furthermore, since a large dipole moment implies a large strength, several two-body bound states will be present. This must be taken into account in simulations of configurations of actual systems where a finite temperature might lead to population of different excited states. In practice, finite temperature in the system will put a natural limit on how small binding energies one needs to consider, i.e. for  $|E| < k_B T$  the bound states are thermally dissociated into the continuum and therefore largely irrelevant.

Second, a positive net volume still allows bound states in two dimensions. However, now it is necessary to have a non-zero minimum attraction where the strength would increase with the net volume. This resembles the situation in three-dimensional quantum mechanics.

Third, the structure of many particles in layers are strongly influenced by their pair interactions. The absence of a critical interaction strength for binding implies that different phases do not exist for different interaction strengths or dipole moments. Therefore a phase transition from a superfluid to a dipolar chain liquid cannot occur in contrast to the suggestion in [11, 16]. Furthermore, the presence of bound states in bilayers for all strengths immediately implies that chains in multilayers will also be present for all couplings. We would therefore expect the system to always be a dipolar chain liquid. As all the individual chains can form immediately the chain-chain interaction becomes interesting and necessary to include in careful future investigations.

We can in fact give an upper bound on the binding energy of a chain of  $M$  particles in  $M$  different layers. The scaling of two-body energy with layer distance is  $E(nd) = E_2/n^2$ , with  $n$  an integer giving the distance in equally spaced layers a distance  $d$  apart. Here  $E_2$  is the two-body energy we have calculated above which depends on the coupling strength. Taking the large  $M$  limit, the upper bound is

$$E_M = E_2 M \sum_{n=1}^{\infty} \frac{1}{n^2} = \frac{\pi^2}{6} M E_2. \quad (14)$$

This estimate of the energy as proportional to the two-body term agrees well with the calculation of [11] where the harmonic approximation was at small couplings for  $M = 2$  and  $M = 81$ .

Fourth, the potential with  $V_{rep}$  in Fig. 1, opposite to  $V_{att}$  can now be created with the use of laser-fields [23,24]. This potential with repulsion at small distance and an intermediate attractive pocket also has at least one bound state for any strength. In the bilayer system with a finite density of fermionic polar molecules in each layer, Ref. [23] found an interesting particle-hole coherent state. The density used there was chosen small so intralayer interaction is negligible and the focus was on the interlayer repulsion corresponding to a barrier at small radii and an attractive pocket outside. In [23] the presence of bound states shown in this paper was ignored. In a real system at finite temperature this coherent state could probably exist at low dipole strength. However, at larger strengths the bound states must be taken into account and one would presumably have instead an interacting gas of bound pairs behaving as a superfluid.

Fifth, the bound states become extremely extended as the energy gets sufficiently close to zero. Such delocalized two-body states can in turn enter into complicated multi-particle complexes. A bound three-body system of two particles in one plane and one in between in the adjacent plane is therefore possible. This presupposes that the repulsive intraplane interaction between these extended structures is less than two times the two-body binding energy that created the two-body bound states. This sort of Y-junction configuration can be very interesting in thermodynamic considerations of chains as it will contribute non-trivially to the entropy and can help lower the free energy. Full quantum studies of such configurations are therefore very relevant and worth pursuing.

Sixth, the optimum conditions for interesting multi-particle structures are probably in the regime close to the threshold for binding of the second state. This can be below the threshold where additional attraction from other particles would lead to binding in analogy to Borromean three-body systems where the two-body subsystems are unbound [17,21]. It can also be for slightly larger attraction and with a bound two-body state since such a system still is spatially extended and in a sense rather similar to the unbound continuum state. The latter case is analogous to the extremely weakly bound atomic helium dimer where the trimer becomes well bound but with a very weakly bound and spatially extended excited state [17,21].

Seventh, the regime of weak binding, strong delocalization and large root-mean-square radius exhibits universal features independent of the shape of the potentials. The same type of universality is likely to exist for multiple bound states but much finer tuning is probably required to reach these structures.

**Conclusions.** — Presently experimentalists are working to produce layered systems of dipolar molecules. We use simple model potentials to study the bilayer case with dipoles polarized perpendicular to the layers. We find the quantum solutions and calculate properties of the wave functions and in particular binding energies and radii as

functions of dipole moment or strength of the potentials. Realistic potentials are used to test the generality of our results.

We conclude that there always is a bound state for all strengths of the dipole-dipole potential. We find that the wave functions of both ground and excited states show universal behavior at zero energy as they basically reside where the potential has become vanishingly small. To access this universal regime the dipole strength must be tuned around the threshold for a bound state to appear. The extended wave functions indicate that three or more particle complexes are possible in chains and in bilayers. The repulsive in-plane interaction becomes interesting in connection with these structures. In any case the tuning of interactions to universal regimes emphasizes the close analogy to the physics studied through the well-known technique of Feshbach resonances.

## REFERENCES

- [1] GRIESMEIER A., WERNER J., HENSLER S., STUHLER J. and PFAU T., *Phys. Rev. Lett.*, **94** (2005) 160401.
- [2] VENGALATTORE M., LESLIE S. R., GUZMAN J. and STAMPER-KURN, D. M., *Phys. Rev. Lett.*, **100** (2008) 170403.
- [3] FATTORI M. ET AL., *Phys. Rev. Lett.*, **101** (2008) 190405.
- [4] POLLACK S. E. ET AL., *Phys. Rev. Lett.*, **102** (2009) 090402.
- [5] OSPELKAUS S. ET AL., *Nature Phys.*, **4** (2008) 622
- [6] NI K.-K. ET AL., *Science*, **322** (2008) 231
- [7] DEIGLMAYR J. ET AL., *Phys. Rev. Lett.*, **101** (2008) 133004.
- [8] LANG F. ET AL., *Phys. Rev. Lett.*, **101** (2008) 133005.
- [9] OSPELKAUS S. ET AL., *Science*, **101** (2010) 853.
- [10] LUSHNIKOV P. M., *Phys. Rev. A*, **66** (2002) 051601
- [11] WANG D.-W., LUKIN M. D. and DEMLER E., *Phys. Rev. Lett.*, **97** (2006) 180413.
- [12] KLAUNN M., DUHME J. and SANTOS L., *Phys. Rev. A*, **81** (2010) 013604
- [13] NOVOSELOV K. S. ET AL., *Nature Phys.*, **2** (2006) 177
- [14] YE J., *Jour. Low Temp. Phys.*, **158** (2010) 882
- [15] YUDSON V. I., ROZMAN M. G. and REINEKER P., *Phys. Rev. B*, **55** (1997) 5214
- [16] WANG D.-W., *Phys. Rev. Lett.*, **98** (2007) 060403.
- [17] A.S. Jensen, K. Riisager, D.V. Fedorov and E. Garrido, *Rev. Mod. Phys.* **76** (2004) 215-261.
- [18] LANDAU L. D. and LIFSHITZ E. M., *Quantum Mechanics* (Pergamon Press, Oxford) 1977.
- [19] SHIH S.-M. and WANG D.-W., *Phys. Rev. A*, **79** (2009) 065603
- [20] TICKNOR C., *Phys. Rev. A*, **80** (2009) 052702
- [21] NIELSEN E., FEDOROV D. V., JENSEN A. S. and GARRIDO E., *Phys. Rep.*, **347** (2001) 373
- [22] ABRAMOWITZ M. and STEGUN I., *Handbook of Mathematical Functions with Formulas, Graphs, and Mathematical Tables* (Dover, New York) 1964.
- [23] LUTCHYN R. M., ROSSI E. and DAS SARMA S., *arxiv:0911.1378v1*, (2009)
- [24] COOPER N. R. and SHLYAPNIKOV G. V., *Phys. Rev. Lett.*, **103** (2009) 155302